DNA-Binding and Oligomerization Studies of the Manganese(II) Metalloregulatory Protein MntR from *Bacillus subtilis*†

Scot A. Lieser,‡ Talib C. Davis,‡ John D. Helmann,§ and Seth M. Cohen*,‡

Department of Chemistry and Biochemistry, University of California at San Diego, La Jolla, California 92093-0358, and Department of Microbiology, Wing Hall, Cornell University, Ithaca, New York 14853

Received June 13, 2003; Revised Manuscript Received August 21, 2003

ABSTRACT: The metalloregulatory protein MntR from *Bacillus subtilis* acts as a transcriptional regulator of manganese homeostasis. MntR is a member of a subfamily of DtxR-related proteins that perform analogous regulatory functions in a variety of pathogenic organisms. Metal ions activate MntR to bind DNA and repress the transcription of the *mntH* gene, which encodes for a proton-coupled metal ion transporter. Size-exclusion chromatography and sedimentation equilibrium ultracentrifugation studies show that apo MntR is predominantly a homodimer in solution. Using fluorescence anisotropy measurements, the DNA binding properties of MntR have been examined. In the strict absence of divalent transition metal ions MntR has a low affinity for the *mntH* control sequence (K_d > 8.0 μM). However, binding of MntR is stimulated by the presence of Mn^{2+} and Cd^{2+} to generate high affinity binding with K_d values of 16.0 and 7.3 nM, respectively. MntR is also shown to bind the *mntH* control sequence in the presence of other divalent transition metals, including Ni^{2+}, Cu^{2+}, and Zn^{2+}, but with much lower affinity ($K_d \approx$ 1.3−2.3 μM). The data here demonstrate that differences in metal-activated DNA binding plays a role in the mechanism of manganese(II)-selective transcription factors and that the oligomerization of MntR is metal-independent, which distinguishes this protein from iron(II)-responsive homologues in the DtxR protein family.

Metal ion homeostasis is a critical factor in the metabolism of all living organisms, from microbes to mammals. A growing area of research in recent years has sought to understand how cells uptake, transport, and traffic the metal ions required for normal metalloprotein function and cell survival (*1*). One of the central components in metal ion homeostasis, particularly for bacteria, are metalloregulatory proteins (*2*, *3*). Metalloregulatory proteins, or simply metalloregulators, are transcription factors that activate or repress operons in response to metal ion concentrations in the cell. Metalloregulators have been portrayed as metal-sensor proteins that act as on/off switches for genes, thereby playing a central role in maintaining cellular metal ion concentrations.

To date, several families of metalloregulatory proteins have been described that respond to both metabolically essential and toxic metal ions including, arsenic (*4*), cadmium (*5*, *6*), cobalt (*7*, *8*), copper (*9*, *10*), iron (*11*−*14*), manganese (*15*−*18*), mercury (*19*), nickel (*7*, *20*, *21*), and zinc (*22*−*27*). Among these proteins, the identification of manganese(II)-stimulated regulators is relatively recent (*15*−*18*). The metalloregulators MntR[1] (*16*), ScaR (*17*), SirR (*18*), and TroR (*15*, *28*) have been described as a manganese(II)-dependent subfamily of the diphtheria toxin repressor (DtxR) class of metalloregulatory proteins (*13*). MntR homologues have been identified in at least three different organisms (*16*, *29*, *30*), including the pathogen *Staphylococcus aureus*, in which MntR modulates oxidative stress resistance via manganese(II) uptake and may play a role in virulence (*30*). Most DtxR-family metalloregulators studied are responsive to iron(II) (*31*), making MntR, ScaR, SirR, and TroR interesting candidates for understanding how the iron-responsive and manganese-responsive members of this protein family elicit distinct metal-specific regulation. To determine the origin of the metal-selective response of these regulatory systems, we have initiated an effort to characterize the oligomerization, metal-binding, and DNA-binding properties of manganese metalloregulatory proteins.

Recent studies have shown that metal specificity in the DtxR-family of proteins appears to be controlled by a combination of factors that include both the nature of the protein metal binding site and the cellular context of the protein (*32*). In complement to these in vivo studies, this report describes in vitro efforts to elucidate the source of the metal-specific response for manganese metalloregulatory proteins. To this end, the expression, purification, oligomerization, and DNA-binding properties of wild-type MntR from

† This work was supported by the University of California, San Diego, the Chris and Warren Hellman Faculty Scholar award (S.M.C.), a Hellman Fellowship (S.M.C.), and NIH Grant Nos. GM-59323 (J.D.H.) and GM-60202-03 (T.C.D.). S.A.L. was supported by the Heme and Blood Proteins Training Program.

* To whom correspondence should be addressed. Telephone: (858) 822−5596. Fax: (858) 822−5598. E-mail: scohen@ucsd.edu.

‡ University of California.

§ Cornell University.

[1] Abbreviations: CD, circular dichroism; DtxR, diphtheria toxin repressor; ICP-OES, inductively coupled plasma optical emission spectroscopy; MALDI-TOF, matrix-assisted laser desorption time-of-flight mass spectrometry; MntR, manganese transport regulator from *B. subtilis*.

10.1021/bi0350248 CCC: $25.00
Published on Web 10/11/2003

Bacillus subtilis (*16*, *32*) is described. The *mntR* gene encodes for a 142-amino acid (~16.7 kDa) DNA-binding protein that shows homology to the DtxR-family of metalloregulatory proteins (*16*, *32*). Size-exclusion chromatography and sedimentation equilibrium ultracentrifugation experiments have been utilized to determine the oligomerization state of apo and metal-bound MntR. In addition, DNA-binding of MntR to the *mntH* recognition sequence was examined by using fluorescence anisotropy experiments. The results suggest activating metal ions belong in two distinct classes: strong activators that induce tight DNA binding and weak activators that produce low affinity DNA binding.

EXPERIMENTAL PROCEDURES

General. All buffers were prepared using water purified through a Labconoco Water Pro Plus purification system. Buffers were degassed and sterilized by passing them through 0.22 μm filters. All biochemical reagents were obtained from commercial suppliers and were used as provided. $MnCl_2 \cdot 4H_2O$, $CdCl_2 \cdot H_2O$, $CuCl_2$, $NiCl_2 \cdot 6H_2O$, and $ZnCl_2$ (99.99+%) were obtained from Aldrich. All protein chromatography was performed at 4 °C on an ÄKTA Prime biomolecule purification system (Amersham Pharmacia Biotech) using both online UV and conductance detection. Matrix-assisted laser desorption time-of-flight (MALDI-TOF) mass spectrometry was performed on a PE Biosystems Voyager-DE STR MALDI-TOF instrument located at the Mass Spectrometry Facility in the Department of Chemistry and Biochemistry at the University of California, San Diego.

Expression and Purification of Wild-Type MntR. BL21-CodonPlus(DE3)-RIL *Escherichia coli* cells (Stratagene) transformed with pET17b plasmid containing the wild-type MntR (*16*) gene were grown in TB media containing ampicillin (100 μg/mL) at 37 °C until the cultures reached an $OD_{595} = 1.0$. The cells were then induced with 1.0 mM IPTG for 3−4 h at 37 °C. The cells were harvested at 12000*g* for 15 min and the pellet was stored at −80 °C until lysis. Cell pellets were resuspended in lysis buffer (50 mM Tris, pH 8.0, 25 °C, 200 mM NaCl, 5 mM EDTA, 5% (v/v) glycerol, 5 mM β-mercaptoethanol). The cell suspension was then lysed by sonication and the lysate was centrifuged twice at 25000*g* for 30 min. The supernatant was applied to a 15-mL anion exchange column (Q Sepharose Fast Flow, 3 × 5 mL, Amersham Pharmacia Biotech) at 4 °C (load 2.0 mL/min; wash with 150 mL lysis buffer; NaCl gradient, 0.2−1.0 M over 100 mL at 5.0 mL/min) that had been preequilibrated with lysis buffer. Fractions containing MntR, as detected by the chromatogram and SDS−PAGE, were pooled and dialyzed (Spectra/Por CE, 5 kDa MWCO or RC, 3.5 kDa MWCO, Spectrum Labs) against 4.0 L of cation exchange column buffer (20 mM HEPES, pH 7.0, 4 °C, 150 mM NaCl, 5% (v/v) glycerol) for 4 h and loaded onto a 30 mL cation exchange column (CM Sepharose, Sigma) at 4 °C (load 2.0 mL/min; wash with 300 mL of 50 mM HEPES pH 7.0, 4 °C, 50 mM NaCl, 5% (v/v) glycerol; NaCl gradient, 0.05−1.0 M over 100 mL at 5.0 mL/min). The combined fractions containing pure MntR as detected on the chromatogram and by SDS−PAGE were pooled and concentrated using a Centricon device (Millipore). The concentrated fractions were dialyzed at 4 °C against 2 × 500 mL storage buffer (20 mM HEPES, pH 7.2, 4 °C, 200 mM NaCl, 5% (v/v) glycerol) with 5.0 g (each change) of Chelex resin (Analytical Grade Chelex 100 Resin, 100−200 mesh, sodium form, Bio-Rad) free floating in the dialysis buffer. MntR was quantified using a calculated extinction coefficient of 18910 M^{-1} cm^{-1} (*33*). The dialyzed protein was divided into aliquots of [MntR] ≈ 100 μM and stored at −80 °C until further use. A typical preparation yielded ~15 mg of protein per 1.0 L of culture. The protein was characterized by MALDI-TOF mass spectrometry, which generated two peaks at 16 630 and 16 763 Da. The calculated molecular weight of MntR is 16 759 Da, suggesting that the peak at 16 630 is MntR with the N-terminal methionine residue truncated.

Inductively Coupled Plasma Optical Emission Spectroscopy. The metal content of all preparations of MntR, ultrapure water, buffers, and metal titrant solutions was determined using a Perkin-Elmer Optima 3000 DV inductively coupled plasma optical emission spectrometer (ICP-OES) located at the Analytical Facility at the Scripps Institute of Oceanography. The instrument was calibrated against a known standard (Instrument Calibration Standard 2, SPEX CertiPrep, Inc.). Metal ion concentrations were monitored using the following wavelengths (nm): Mn 257.610, 260.568, 294.920; Fe 238.204, 239.562, 259.939, 273.955; Co 228.616, 230.786, 231.160, 236.380, 238.892; Ni 221.648, 231.604; Cu 224.700, 324.752, 327.393; Zn 202.548, 206.200, 213.857; Cd 228.802, 214.440, 226.502. Ultrapure water and stock buffer solutions routinely contained less than 2 ppb of Mn, Fe, Co, Ni, Cd, 4 ppb of Cu, and 10 ppb of Zn. Concentrations of metal titrant solutions were determined by ICP-OES and consistently showed less than 2 ppb of any metal ion other than the desired cation. Typical protein preparations were confirmed by ICP-OES to contain < 0.001 mol of Mn, Fe, Co, Cd, < 0.01 mol of Ni, Cu, and < 0.06 mol of Zn per mole of MntR monomer.

Circular Dichroism Spectroscopy. Circular dichroism (CD) measurements were made on an AVIV Circular Dichroism model 202 spectrometer using a 2.0-mm quartz cuvette. The cuvettes were washed with 1% Helmenex (80 °C for 10 min), 500 mM HCl, and copious amounts of ultrapure water to ensure the cells were clean and free of metal contaminants. Two 500 μL aliquots of 20 μM MntR were stored at 4 and 25 °C, respectively, for 3 days. CD spectra (185−300 nm) were collected at 0, 24, 48, and 72 h for each sample with a 1.0-nm step, 1.0 s averaging time, at 25 °C (temperature controlled cell jacket).

Size-Exclusion Chromatography. A HiLoad 16/60 Superdex 75 Size Exclusion column (Amersham Pharmacia Biotech) was calibrated with a Low Molecular Weight Calibration kit (Amersham Pharmacia Biotech) consisting of four proteins with a MW range of 13.7−67 kDa, plus Blue Dextran 2000 to measure the void volume. The resulting calibration plot of K_{av} ($K_{av} = (V_e - V_o)/(V_t - V_o)$, where V_e = protein elution volume, V_o = column void volume = 43.3 mL, and V_t = total bed volume = 124.5 mL) vs MW was fit with the equation $y = -0.1963 \ln(x) + 2.3287$ ($R^2 = 0.9995$). MntR protein samples (500 μL aliquots of 54.3 μM MntR) were dialyzed overnight against storage buffer at pH 7.2, 7.4, 7.6, 7.8, and 8.0. The dialyzed samples were then applied to the calibrated column and run at a flow rate of 1 mL/min. Under these conditions, MntR elutes as a single peak with a maxima at ~67 mL, corresponding to an apparent molecular mass of ~32 kDa.

Analytical Sedimentation Equilibrium Ultracentrifugation. Sedimentation experiments were performed on a Beckman XL-1 Analytical ultracentrifuge located at the Biophysics Instrumentation Facility in the Department of Chemistry and Biochemistry at the University of California, San Diego. Experiments were performed at 20 °C using an An-60 Ti rotor and a six-channel centerpiece with sapphire windows and a path length of 1.2 cm. Prior to sample addition, the cells were thoroughly washed with ~1.0 M HCl followed by copious amounts of metal-free ultrapure water and buffer to minimize any potential metal contaminants. Equilibrium sedimentation experiments were performed at apo MntR concentrations of 5−35 μM (corresponding to $OD_{280} \approx 0.10-0.60$) diluted in storage buffer. Apo MntR data was collected at speeds of 20 000, 25 000, and 35 000 rpm to ensure the protein oligomerization state was independent of rotor speed. In addition to absorbance data, interferometry data was collected for some experiments. Metal-containing MntR samples were prepared as above with an MntR concentration of 5 μM and 1 equiv of Mn^{2+}, Cd^{2+}, Zn^{2+}, Ni^{2+}, or Cu^{2+} and were run at 35 000 rpm. Data were analyzed by using the nonlinear least-squares fitting software program Microcal Origin and macros for this program supplied by Beckman-Coulter. To obtain an apparent molecular weight the data were fit to eq 1:

$$A_r = A_0 \exp[HM(x^2 - x_0^2)] + E \quad (1)$$

where

$$H = (1 - \upsilon\rho)\omega^2/2RT$$

and A_r = absorbance at radius x, A_0 = absorbance at the reference radius x_0, M = molecular weight, E = baseline offset, υ = partial specific volume of MntR (0.741 mL/g, calculated using Sednterp), ρ = solvent density (1.035 g/mL), and ω = angular velocity. To obtain self-association constants for the MntR monomer ↔ dimer equilibrium the data were fit to eq 2:

$$A_{r,total} = A_0 \exp[HM(x^2 - x_0^2)] + (A_0)^{n_2} K_{assoc} \exp[HMn_2(x^2 - x_0^2)] + E \quad (2)$$

where M = monomer molecular weight, n_2 = stoichiometry (2 for homodimer), and K_{assoc} = association constant for the monomer ↔ dimer equilibrium. Association constant values in absorbance units were converted to units of M^{-1} using an $\epsilon_{280} = 18910\ M^{-1}\ cm^{-1}$ and a cell path length of $l = 1.2$ cm.

Fluorescence Anisotropy Titrations. Fluorescently labeled oligonucleotides were purchased from Integrated DNA Technologies (Coralville, Iowa). An oligonucleotide containing a 5′ fluorescein label was obtained with the following sequence: 5′-6F-GAATAATTTGCCTTAAGGAAACTCTC-3′ (ss*mntH*26), where the fluorescein dye is indicated by 6F (6F = 6-carboxyfluorescein). The oligonucleotide ss*mntH*26 was annealed with 1.1 equiv of a complementary oligonucleotide (5′-GAGAGTTTCCTTAAGGCAAATTATTC-3′) to generate the double-stranded oligonucleotide ds*mntH*26 containing the desired recognition sequence. The ds*mntH*26 sequence was annealed by heating the reaction mixture to 95 °C followed by slow cooling to room temperature in a buffer containing 10 mM Tris (pH 7.5), 50 mM NaCl, and 10 mM $MgCl_2$.

Fluorescence anisotropy measurements were performed by using a Perkin-Elmer Luminescence spectrometer LS 50B using an excitation wavelength of 475 nm (slit width 15 nm), an emission wavelength of 525 nm (slit width 20 nm), and a 1.0 s integration time. A 1.0-cm near-UV quartz cuvette (Wilmad) was placed in a thermally jacketed cell holder that was maintained at 25 °C. The initial solution was mixed using a small magnetic stir bar and allowed to temperature equilibrate for at least 10 min before any measurements were collected. Slow stirring was maintained throughout the titration. The g-factor was calculated by using the instrument software for each set of solution conditions (e.g., different metal ions) and was then kept constant for each replicate under the same conditions. The g-factor for all of the experiments was 1.03 ± 0.01.

In a typical titration a 2.0-mL solution was placed in the cuvette (prewashed with water, 500 mM HCl, and EtOH between each titration) containing 20 mM HEPES (pH 7.2, 4 °C), 500 mM NaCl, 5% (v/v) glycerol, and either 2 nM (for Cd^{2+} and Mn^{2+} titrations) or 100 nM (for apo, Cu^{2+}, Ni^{2+}, and Zn^{2+} titrations) of ds*mntH*26. For titrations in the presence of metal ion, the latter solution would also contain 1.0 mM of the appropriate metal ion. Titrant solutions containing between 0.4 nM − 100 μM apo MntR were added to the cuvette in 5−50 μL aliquots, never exceeding 5% of the total solution volume (except in the case of Zn^{2+}, where a total of 265 μL of titrant was added). For titrations using stoichiometric amounts of metal ion, either one or two molar equivalents of the metal salt was preincubated with the protein titrant for at least 2 h at 4 °C. A zero-point measurement (no added protein) was acquired at the beginning of each titration to establish a baseline anisotropy measurement. After each addition of protein the mixture was allowed to equilibrate for 30 s and then 5−8 measurements were taken and averaged. The r_{obs} versus $[MntR]_{total}$ data were fit either to a 1:1 binding isotherm model (nondissociable dimer) by using least-squares regression analysis software (MicroCal Origin, Synergy KaleidaGraph) or were coupled to the dimer ↔ monomer equilibrium ($K_{dimer} \approx 175$ nM, based on sedimentation equilibrium ultracentrifugation experiments) by using the software DYNAFIT (*34*). Data reported (vide infra) are based on the nondissociable dimer model.

RESULTS

Preparation and Characterization of MntR. Wild-type MntR was purified using a series of ion-exchange columns. This procedure provides a yield of approximately ~15 mg of protein per liter of culture. The protein was isolated to >95% homogeneity as determined by densitometry of denaturing polyacrylamide gels stained with Coomasie Brilliant Blue (Figure S1, Supporting Information). Circular dichroism (CD) spectroscopy of the purified protein shows (Figure 1) the protein has substantial α-helical content as expected by homology to the structurally characterized DtxR proteins. The prominent feature at 222 nm is characteristic of the anticipated α-helical regions (*35*). The stability of the purified protein was also probed using CD spectroscopy. Two separate protein aliquots were stored at 4 and 25 °C, and their CD spectra were measured after 0, 24, 48, and 72 h.

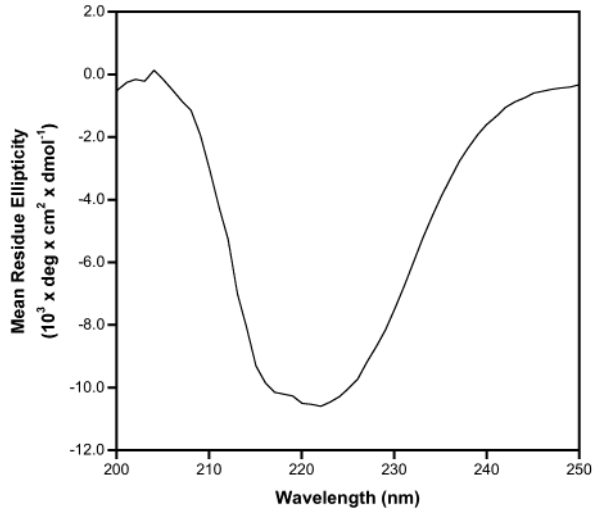

FIGURE 1: Circular dichroism (CD) spectra of wild-type MntR. [MntR] = 46 μM. Buffer = 20 mM HEPES (pH 7.2), 200 mM NaCl, 5% (v/v) glycerol. T = 25 °C. Path length = 2 mm.

The spectra were invariant of temperature and time, which indicates that the protein is quite stable at ambient temperature for several days. This was also confirmed by SDS−PAGE analysis of the same samples after 72 h, which indicated that no proteolysis of the protein had occurred over this same time period (data not shown). These experiments demonstrated the protein was sufficiently stable to perform equilibrium sedimentation (vide infra) and other experiments. Addition of Mn^{2+} to solutions of MntR did not produce significant changes in the CD spectrum of the protein (data not shown), suggesting that metal binding does not induce significant secondary structure changes.

Oligomerization State of MntR. Using a calibrated size-exclusion column an apparent molecular weight for MntR was determined. With an elution volume maximum of ~67 mL, a molecular mass of ~32 kDa is obtained, consistent with dimeric MntR being the predominant species in solution (Figure S2). During purification optimization, aggregation of MntR had been observed under conditions of high pH (Tris, pH ~8.6). Therefore, the pH dependence of the size-exclusion chromatogram was examined under the finalized purification conditions. No deviation in the elution profile of the dimer was found over a pH range of 7.2−8.0 (20 mM HEPES, 4 °C). Therefore, under the present conditions the homodimer state of the protein is stable over nearly one entire pH unit.

Analytical ultracentrifugation (*36*) techniques provide powerful tools for the analysis of metalloregulatory protein solution behavior (*5*, *37*, *38*). Therefore, as further evidence of the oligomerization state of apo MntR, sedimentation equilibrium experiments were performed. Representative absorbance data of apo MntR are shown in Figure 2. Fitting to a single, ideal species (eq 1) gave an apparent molecular mass of ~33081 Da (Table 1), which is in excellent agreement with the expected molecular weight of an MntR homodimer (16759 Da × 2 = 33518 Da) and is consistent with the size exclusion chromatography data. Interferometry measurements were collected on selected sedimentation experiments; when fit to eq 1 these data also gave molecular weight values indicating apo MntR was a homodimer in solution (data not shown).

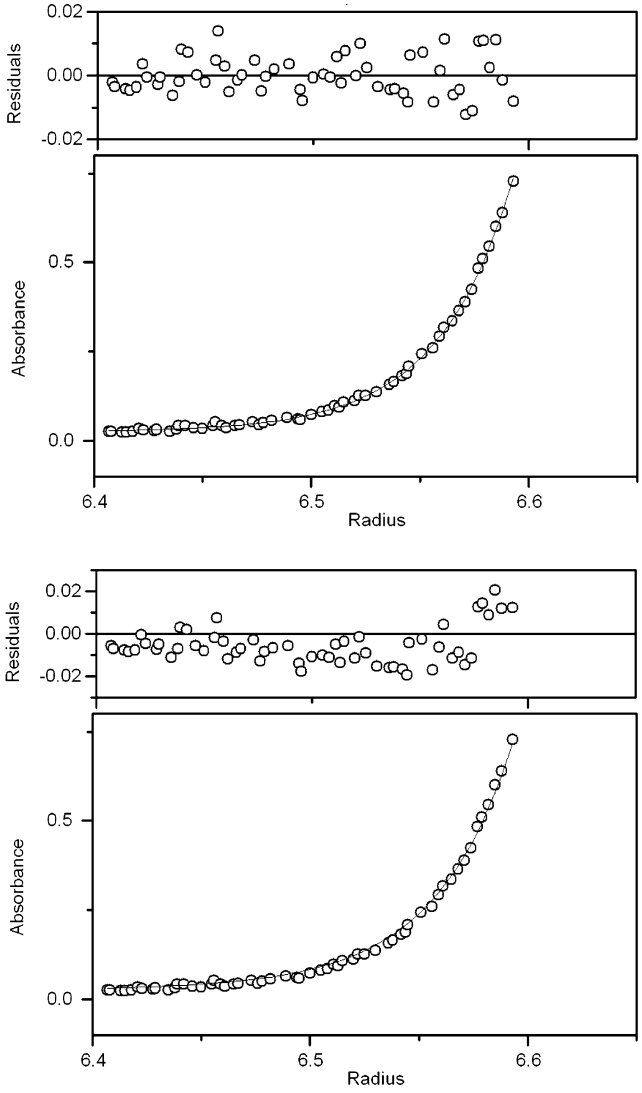

FIGURE 2: Ultracentrifugation data for apo MntR monitored by absorbance at 280 nm. The line through the data is a nonlinear least-squares fit from which the apparent molecular weight (top) and dimerization constant (bottom) was obtained. [MntR] = 25 μM. Buffer = 20 mM HEPES (pH 7.2), 200 mM NaCl, 5% (v/v) glycerol. T = 20 °C.

Table 1: Analytical Ultracentrifugation Sedimentation Equilibrium Data Results Based on a Fit to Eq 1 (MW) or Eq 2 (K_{dimer})[a]

[MntR] (μM)	MW (Da)	K_{dimer} (nM)
5	32799 ± 2	153 ± 28
15	35810 ± 191	111 ± 47
25	33491 ± 963	203 ± 56
35	30224 ± 668	231 ± 17
5 (+Mn^{2+})	34208 ± 1042	113 ± 31
5 (+Cd^{2+})	33124 ± 6	244 ± 53
5 (+Cu^{2+})	34672 ± 392	105 ± 23
5 (+Ni^{2+})	33929 ± 871	115 ± 26
5 (+Zn^{2+})	35177 ± 1065	123 ± 28

[a] All values are based on an average of at least three independent experiments. Buffer = 20 mM HEPES (pH 7.2), 200 mM NaCl, 5% (v/v) glycerol. Rotor speed = 35 000 rpm. T = 20 °C.

The fit to a single idealized species generated a molecular weight in good agreement with an MntR homodimer, suggesting there was very little MntR monomer in solution and that the dimer ↔ monomer equilibrium was substantially shifted toward dimer formation. Therefore, sedimentation

equilibrium experiments were also used to measure the self-association/dimerization constant (hereon referred to as K_{dimer} and reported in terms of a dissociation constant) by fitting the absorbance data to eq 2. When fitting the data using this model, the monomer molecular mass was fixed at 16759 Da and only K_{dimer} was allowed to vary (Figure 2). The data indicate, as expected from the molecular weight fits, apo MntR forms a tight homodimer with a K_{dimer} of ~175 nM (Table 1), which may be an upper limit for this value (vide infra).

The effect of metal ions on the dimerization of MntR was also examined. At MntR concentrations of greater than 5 μM, the addition of one or more equivalents (per MntR monomer) of Ni^{2+} or Zn^{2+} resulted in protein precipitation. Addition of Mn^{2+} under these conditions did not cause visible precipitation; however, the resulting sedimentation equilibrium experiments indicated protein aggregation (data not shown). This precipitation/aggregation problem, under the solution conditions used, strictly limited the ability to examine the influence of metal ions by analytical ultracentrifugation. However, at an MntR concentration of 5 μM, satisfactory data could be obtained in the presence of one equivalent of Mn^{2+}, Ni^{2+}, Cu^{2+}, Zn^{2+}, and Cd^{2+}. The data are summarized in Table 1 and indicate that under these conditions the presence of divalent metal ions does not significantly change the K_{dimer} for MntR. Addition of one equivalent of Mn^{2+} or other divalent transition metals at low protein concentrations may have little effect on the oligomerization equilibrium of wild-type MntR. However, based on the low K_{dimer} value obtained for the apo protein, the amount of monomeric MntR is extremely small and changes in this equilibrium may well be undetectable under the present experimental conditions (*39*).

DNA Binding of MntR. Fluorescence anisotropy has proven to be an extremely useful tool for the study of various protein−ligand interactions (*40*). The technique has been very successful for examining the binding of several metalloregulatory proteins to their cognate sequences (*5*, *6*, *41*, *42*). Therefore, using a 26-base pair oligonucleotide (ds*mntH*26) containing the *mntH* recognition sequence and a single fluorophore on the 5′ end of one strand of the DNA, the binding of wild-type MntR in the absence and presence of various first row transition metal ions was examined. The *mntH* recognition sequence is a previously identified binding region for MntR that contains an imperfect palindrome (5′-TTTGCCTTAAGGAAAC-3′) and has substantial similarity to the TroR binding element (*16*). Interestingly, the *mntH* sequence has greater similarity with the consensus sequence of the metalloregulatory protein Fur than that of DtxR (*15*). Solutions of the fluorophore labeled ds*mntH*26 were titrated with increasing amounts of protein. To examine the effects of metal ions, a large excess (1.0 mM) of the metal ion was added to the DNA solution prior to protein addition. A high salt concentration (0.50 M NaCl) was required to reduce the affinity of metal-activated MntR for this sequence and to obtain satisfactory equilibrium data.

In the strict absence of transition metal ions, MntR was found to have a very low affinity for ds*mntH*26, with no binding detected at protein concentrations as high as 8.0 μM (Figure 3). However, upon addition of excess Mn^{2+} (1.0 mM) to the same solution rapid, tight binding was observed. Binding of MntR to ds*mntH*26 was carried out with five

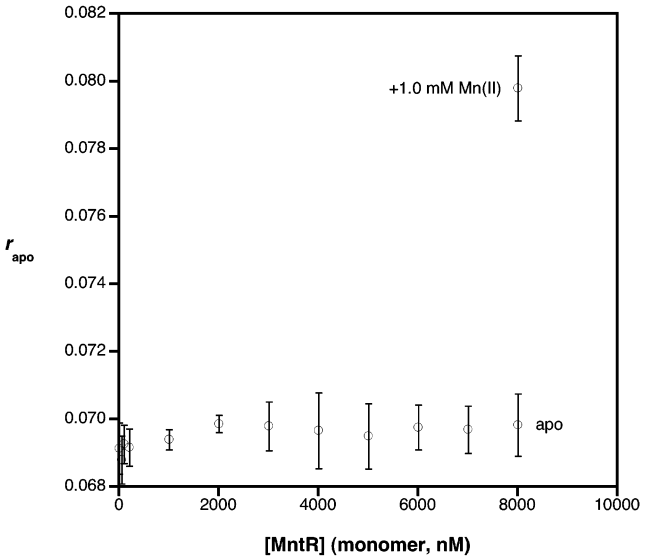

FIGURE 3: Fluorescence anisotropy data for wild-type MntR binding to oligonucleotide ds*mntH*26. No binding is observed in the absence of transition metal ions even at high concentrations of apo MntR. The last two data points are at the same concentration of protein ([MntR] = 8.0 μM), but the upper point is after addition of 1.0 mM Mn^{2+}. Buffer = 20 mM HEPES (pH 7.2), 500 mM NaCl, 5% (v/v) glycerol. [ds*mntH*26] = 100 nM. T = 25 °C.

different transition metal ions: Mn^{2+}, Ni^{2+}, Cu^{2+}, Zn^{2+}, and Cd^{2+} (Figure 4). In each case, an excess (1.0 mM) of metal ion was used; therefore, the precise metal content of MntR under these conditions is not rigorously known. Under such conditions all high affinity, and presumably biologically relevant, as well as any low affinity sites are occupied. Binding assays in the presence of one or two equivalents of Mn^{2+}, Ni^{2+}, or Cd^{2+} generated data similar to that obtained for the apo protein (Figure S3). However, DNA binding in the presence of excess metals clearly revealed that MntR could be activated by all of the aforementioned metal ions to some degree. Two general groups were readily distinguished as strong and weak activators. Mn^{2+} and Cd^{2+} resulted in the highest affinity binding, with K_d values of 16.0 and 7.3 nM, respectively (Table 2). These results are consistent with earlier described electrophoretic mobility shift assays that identified both Mn^{2+} and Cd^{2+} as activators of MntR (*16*). In addition, Ni^{2+}, Cu^{2+}, and Zn^{2+} were identified as weak activators generating only modest, but significant binding, when compared to apo protein. In the presence of Cu^{2+}, a dissociation constant of ~1300 nM was obtained, while Ni^{2+} and Zn^{2+} showed weaker activation with K_d values ~2300 nM. This effect was not due simply to the presence of high concentrations of any divalent cation, as titrations in the presence of 1.0 mM Ca^{2+} and Mg^{2+} showed no significant DNA binding (data not shown), identical to that observed with apo protein.

The stoichiometry of the protein−DNA complex was determined by the mole ratio method (*43*, *44*); a titration with 1.0 mM Mn^{2+} was performed as previously described, but in the presence of 100 nM instead of 2.0 nM *dsmnt*H26. Under these conditions, every addition of protein results in nearly complete formation of the protein−DNA assembly, and saturation is observed with a break point at ~2.1 equiv of MntR per equiv of *dsmnt*H26 (Figure S4), consistent with the binding of one MntR dimer for each oligonucleotide.

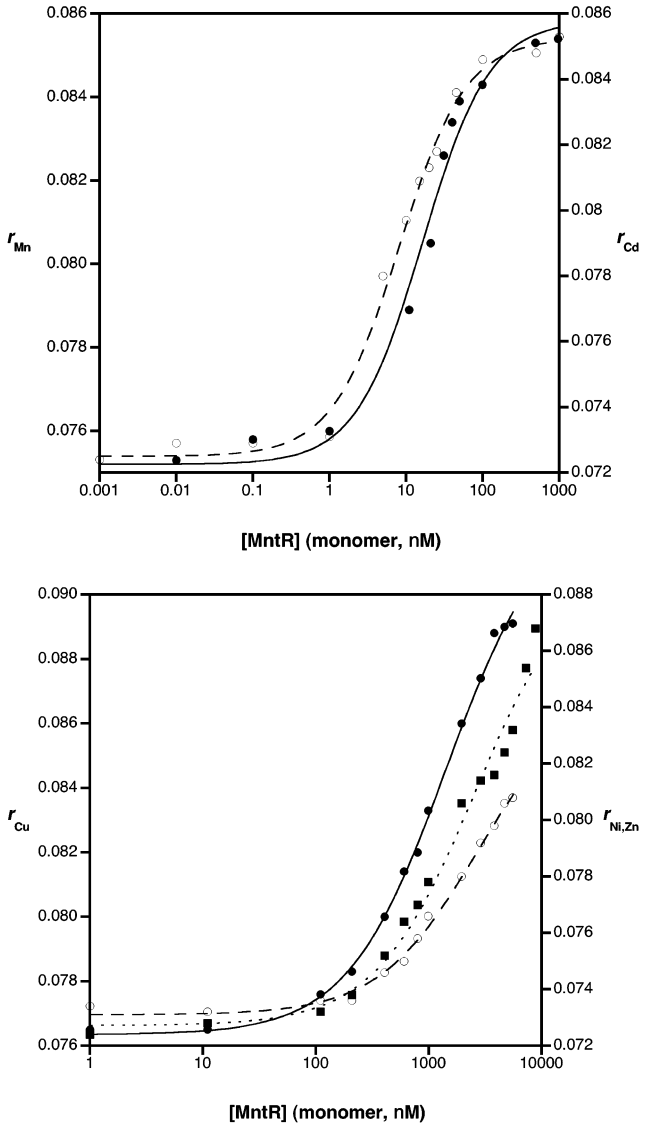

FIGURE 4: Representative fluorescence anisotropy data for wild-type MntR binding to the oligonucleotide ds*mntH*26. High affinity binding (top) is demonstrated in the presence of 1.0 mM Mn^{2+} (filled circles) and Cd^{2+} (open circles) ([ds*mntH*26] = 2.0 nM). Significantly weaker binding (bottom) is found in the presence of 1.0 mM Cu^{2+} (filled circles), Ni^{2+} (open circles), and Zn^{2+} (filled squares) ([ds*mntH*26] = 100 nM). Lines through each set of points represent a fit of the data to a 1:1 oligonucleotide/dimer binding isotherm. Buffer = 20 mM HEPES (pH 7.2), 500 mM NaCl, 5% (v/v) glycerol. T = 25 °C.

All of the K_d values reported were obtained from fitting the fluorescence anisotropy data to a simple 1:1 binding isotherm (Figure 4), which gave excellent correlations with the experimental data (Table 2). However, due to the very high affinity of MntR for ds*mntH*26 in the presence of Mn^{2+} and Cd^{2+}, the binding equilibria under these conditions should be highly correlated with the dimer ↔ monomer equilibria based on the values obtained in sedimentation equilibrium experiments (*5*, *6*, *41*, *42*). Therefore, all of the fluorescence anisotropy data were analyzed using the program DYNAFIT (*34*) using models with and without coupling to the dimerization equilibrium. The result of these analyses were that coupling the protein oligomerization to the DNA binding equilibrium did not significantly improve the quality of the fits. There are several possible explanations for why DNA binding does not appear to be influenced by the dimerization reaction (vide infra), but ultimately it does not alter the overall results from the fluorescence anisotropy experiments. Although the absolute binding constants will change based on whether protein oligomerization is accounted for or not, the trend in relative binding constants remains essentially the same, with a variety of first row transition metal ions being capable of activating MntR; Mn^{2+} and Cd^{2+} affect high affinity binding, while Ni^{2+}, Cu^{2+}, and Zn^{2+} generate low affinity binding to DNA.

Table 2: Dissociation Constants (K_d) and Quality-of-Fit Parameters for Modeling the Fluorescence Anisotropy Data with a 1:1 Binding Isotherms[a]

metal ion (1 mM)	K_d (nM)	correlation coefficient (R)[b]	χ^2 [c]
apo	>8000 (estimated)	N/a	N/a
Mn^{2+}	16.0 ± 0.4	0.995	2.05
Cd^{2+}	7.3 ± 1.1	0.991	5.76
Cu^{2+}	1308 ± 87	0.999	0.560
Ni^{2+}	2342 ± 305	0.997	0.573
Zn^{2+}	2337 ± 168	0.990	6.07

[a] All values are based on an average of at least three independent experiment. [b] $R = \sum_i (x_i - \bar{x})(y_i - \bar{y})/(\sqrt{\sum_i (x_i-\bar{x})^2}\ \sqrt{\sum_i (y_i-\bar{y})^2})$. [c] $\chi^2 = \sum_i (y_i - f(x_i)/\sigma_i)^2$.

DISCUSSION

Size-exclusion chromatography and sedimentation equilibrium experiments clearly support the conclusion that apo wild-type MntR is a homodimer with a predicted molecular mass of 33 518 Da in its native state. The equilibrium constant for the homodimerization has been determined to be $K_{dimer} \approx 175$ nM or lower, indicating the dimer is the dominant form of the protein in solution. These sedimentation equilibrium data are consistent with earlier studies on manganese(II) metalloregulatory proteins suggesting a homodimeric native state (*15*, *16*). However, these findings are in marked contrast to DtxR-family proteins that belong to the traditionally iron-responsive group (*31*). Earlier studies on DtxR established that homodimerization is required for DNA binding, and this process was mediated by metal complexation (*45*). A more recent study suggests DtxR may form a dimer with self-association constants around the micromolar range that is further lowered to ~33 nM upon metal complexation (*46*). This apparent difference in oligomerization behavior prompts the question of how and why do DtxR and MntR, and perhaps most iron versus manganese-responsive DtxR-family metalloregulators, maintain different quaternary structures in the absence of metal ions?

An examination of the proposed dimerization domain for MntR, based on sequence alignment and structural data from the metalloregulatory proteins DtxR (*47*−*51*) and IdeR (*52*) does show significant differences between the iron- and manganese-responsive proteins (Figure 5). The amino acids that contribute to the dimerization interface for DtxR and IdeR are defined as 21 residues, namely, 85−91 and 103−116 (*51*), which corresponds to residues 83−88 and 100−113 in MntR (*16*). DtxR and IdeR share 17 identical and four conserved amino acids in this dimerization region, and this high degree of similarity appears to be generally true for related iron-dependent transcription repressors. In contrast, MntR shares less than half (seven residues) in

```
              85   91 / 103        116
DtxR          LLTDIIG / RWEHVMSDEVERRL
IdeR          LLVDVIG / RWEHVMSEDVERRL
ScaR          FLVHHLG / VLEHTVSDHFVERL
SirR          FLIEILQ / ILEHRISDLFVERL
TroR          FLSQVLC / MLEHACSDELIDVI
MntR          FLR-IIG / GIEHHLSWNSIDRI
              :*   :      **  *      :
```

FIGURE 5: Sequence alignment (ClustalW) for several DtxR family metalloregulatory proteins of the proposed dimerization interface. Absolutely conserved (*) and semi-conserved residues (:) are indicated at the bottom of the alignment. Numbering scheme shown for DtxR. The known Fe^{2+} regulators DtxR and IdeR show extremely high conservation relative to MntR.

common with DtxR in these regions. This is quite representative of all the characterized manganese(II)-responsive repressors which possess only four conserved and three semi-conserved residues in this area when compared with DtxR. Additionally, of these seven residues only four (residues 85, 86, 90, and 116, DtxR numbering) are part of the hydrophobic interface between the protein subunits as determined by crystallographic studies (*51*). This analysis indicates there is sufficient variance between the dimerization interfaces of the iron- and manganese-responsive DtxR proteins to generate the divergent oligomerization properties observed for MntR.

Recently, a 1.75 Å resolution crystal structure of wild-type MntR complexed with Mn^{2+} has been solved (*35*). The structure shows two manganese(II) ions bound per MntR monomer; the affinity of Mn^{2+} for these sites and the mechanistic importance of each site has not yet been determined. However, this structure shows an important feature that likely contributes to the strong dimerization of manganese(II)-responsive proteins. Unlike the structures of DtxR and IdeR, the two monomer subunits share an additional α-helical region, Asp123 to Lys136, at the dimerization interface. These α-helices span from one monomer across to the other, and although the details of these interactions have not yet been fully described, it is quite apparent from visual inspection that a significant amount of additional surface contact between the subunits is present that could promote stronger self-association. Further structural, mutagenesis, and biochemical studies will be required to elucidate the details of why dimerization is so strong in MntR, and how loss of this allosteric control feature affects the mechanism of transcriptional and subsequently metal ion regulation by these proteins. Overall, the oligomerization behavior of MntR is distinct in the context of the DtxR-family of metalloregulators, and suggests the mechanism of metal-selective repression for MntR may differ significantly from other members of this protein group.

The fluorescence anisotropy data presented here indicate a variety of transition metal ions can activate MntR. On the basis of the results of the sedimentation equilibrium experiments, the DNA binding equilibrium should be strongly coupled to the dimerization equilibrium (*5*, *6*, *41*, *42*). However, fitting the data with a model that employed a dissociable dimer with a fixed K_{dimer} did not significantly improve the quality of the fits over those using a nondissociable dimer model. There are several potential explanations for this apparent incongruity. One possibility is the self-association constant for MntR is higher than the value determined in the sedimentation equilibrium experiments. Under the experimental conditions, with the detection wavelength employed, the values obtained are essentially at the limit of detection for the instrument (*39*). Therefore, the K_{dimer} ascertained may represent only the upper limit, with the actual value being significantly lower. Another possible explanation can be assigned to the apparent oligomerization/aggregation observed for MntR at higher metal ion concentrations (vide supra). The fluorescence anisotropy experiments were performed in the presence of a large excess of metal ion, which may have altered the aggregation state of MntR in a manner not readily observed under the conditions of the sedimentation equilibrium experiments. Finally, the fluorescence anisotropy measurements were performed at a significantly higher salt concentration (500 nM) than the sedimentation equilibrium studies (200 nM). This was required to reduce the affinity of metal activated MntR for the 26-base pair oligonucleotide used in the fluorescence anisotropy experiments. The difference in salt concentrations, which can affect both protein−protein and protein−DNA interactions, may also contribute to the discrepancy in the binding model. Nevertheless, all of the titrations performed fit well with a simple 1:1 (DNA/MntR dimer) binding isotherm model, with the assumption that MntR was binding as a nondissociable homodimer. In addition, invoking higher order complexes (e.g., 1:2 DNA/MntR dimer, multiple homodimers bound) did not improve the quality of the model.

The trend in DNA binding ability was found to be $Cd^{2+} > Mn^{2+} \gg Cu^{2+} > Zn^{2+} \geq Ni^{2+} \gg$ apo. Mn^{2+} and Cd^{2+} clearly activate MntR more effectively when compared with Cu^{2+}, Ni^{2+}, and Zn^{2+}. Nevertheless, Cu^{2+}, Ni^{2+}, and Zn^{2+} do stimulate MntR to bind DNA at least severalfold more tightly over the apo, Mg^{2+}, or Ca^{2+} saturated forms of the protein. The observation that Mn^{2+} and Cd^{2+} activate the protein with essentially the same efficacy is a particularly curious result of these experiments. Typically, Mn^{2+} and Cd^{2+} are considered to be dissimilar metal ions (*53*, *54*), each behaving as a prototypical hard and soft ion, respectively. How and why MntR responds so effectively to these very different metal ions will be the subject of further examination. The results obtained here are notable in light of the fact that MntR represses MntH, which is known to be the major transporter for both Mn^{2+} and Cd^{2+} at high ambient metal ion concentrations (*16*). Indeed, *mntH* mutants are cadmium resistant (*16*), thus the ability of MntR to be activated by Cd^{2+} may be physiologically advantageous. Under the experimental conditions used here, specifically in the presence of excess metal ion, the differences between the ability of the metal ions examined to activate MntR cannot be definitively assigned. One possible explanation is that only Mn^{2+} and Cd^{2+} cause the most favorable structural changes in MntR to exhibit tight binding. Cu^{2+}, Ni^{2+}, and Zn^{2+} may induce different structural alterations in MntR that are suboptimal for DNA binding. If such a large change in protein structure is occurring, it likely occurs at the tertiary or quaternary level based on the CD spectra reported here that show little or no change in secondary structure upon

addition of Mn^{2+} to MntR. This is consistent with the favored "hinge" or "caliper" mechanism described for DtxR (*47*, *48*, *52*), which involves an adjustment in orientation between the two monomer subunits upon metal binding. Another possible explanation for the variation in metal activation is a difference in the affinity of MntR for each metal ion examined. All of these metals may produce the same or similar structural changes in MntR that trigger DNA binding, but Cu^{2+}, Ni^{2+}, and Zn^{2+} might have significantly lower affinities for the MntR binding site, and therefore the differences observed in the experiments here may be more a reflection of protein−metal affinity than protein−DNA affinity. DNA binding assays performed in the presence of stoichiometric amounts of Mn^{2+}, Ni^{2+}, and Cd^{2+} (Figure S3) do not show binding by MntR to the oligonucleotide probe, suggesting the metal ions are largely dissociated from the protein under these experimental conditions. It is possible that elements of both aforementioned mechanisms are involved, and further experiments to determine the affinity of MntR for various metal ions as well as more DNA-binding experiments performed under stoichiometric or sub-stoichiometric metal ion concentrations will be required.

In summary, a detailed biophysical study of the manganese(II)-dependent metalloregulatory protein MntR from *B. subtilis* is described. MntR is shown to form a tight homodimer in the absence of metal ions, which can be understood in the context of recent structural results. Consistent with earlier studies, MntR is shown to be strongly activated for DNA binding in the presence of excess Mn^{2+} and Cd^{2+}. In addition, Cu^{2+}, Ni^{2+}, and Zn^{2+} are also found to stimulate DNA binding by MntR, but with ∼1000-fold lower affinity. Continuing studies will be focused on determining the precise mechanism by which MntR is activated by these various metal ions and a better understanding the regulatory differences between MntR and iron-responsive members of the DtxR protein family.

ACKNOWLEDGMENT

We thank Prof. Arthur Glasfeld (Reed College) and Prof. Richard G. Brennan (Oregon Health and Science University) for sharing the preliminary MntR crystal structure, Dr. Emmanuel Guedon (Helmann Lab, Cornell University) for providing the MntR vector, Mr. John Croy and Prof. Elizabeth Komives (U.C. San Diego) for assistance with use of the analytical ultracentrifuge and MALDI-TOF mass spectrometer, Ms. Susan Seaman, Mr. Qi Liu, and Prof. Yitzhak Tor (U.C. San Diego) for access and assistance with their fluorimeter, Dr. Kevin Walda (Scripps Institute of Oceanography) for access and assistance with the ICP-OES, and Prof. Partho Ghosh (U.C. San Diego) and Prof. Gouri Ghosh (U.C. San Diego) for helpful discussions.

SUPPORTING INFORMATION AVAILABLE

SDS−PAGE analysis of MntR purification, size exclusion column chromatogram for apo MntR, sub-stoichiometric metal fluorescence anisotropy titrations, and stoichiometric protein fluorescence anisotropy titrations. This material is available free of charge via the Internet at http://pubs.acs.org.

REFERENCES

1. Finney, L. A., and O'Halloran, T. V. (2003) *Science 300*, 931−936.
2. Outten, F. W., Outten, C. E., and O'Halloran, T. V. (2000) in *Bacterial Stress Responses* (Storz, G., and Hengee-Aronis, R., Eds.) pp 145−157, ASM Press, Washington, DC.
3. O'Halloran, T. V. (1993) *Science 261*, 715−730.
4. Wu, J., and Rosen, B. P. (1993) *J. Biol. Chem. 268*, 52−58.
5. Busenlehner, L. S., Cosper, N. J., Scott, R. A., Rosen, B. P., Wong, M. D., and Giedroc, D. P. (2001) *Biochemistry 40*, 4426−4436.
6. Busenlehner, L. S., Apuy, J. L., and Giedroc, D. P. (2002) *J. Biol. Inorg. Chem. 7*, 551−559.
7. Cavet, J. S., Meng, W., Pennella, M. A., Appelhoff, R. J., Giedroc, D. P., and Robinson, N. J. (2002) *J. Biol. Chem. 277*, 38441−38448.
8. Rutherford, J. C., Cavet, J. S., and Robinson, N. J. (1999) *J. Biol. Chem. 274*, 25827−25832.
9. Outten, F. W., Outten, C. E., Hale, J., and O'Halloran, T. V. (2000) *J. Biol. Chem. 275*, 31024−31029.
10. Munson, G. P., Lam, D. L., Outten, F. W., and O'Halloran, T. V. (2000) *J. Bacteriol. 182*, 5864−5871.
11. Bagg, A., and Neilands, J. B. (1987) *Biochemistry 26*, 5471−5477.
12. Althaus, E. W., Outten, C. E., Olson, K. E., Cao, H., and O'Halloran, T. V. (1999) *Biochemistry 38*, 6559−6569.
13. Schmitt, M. P., Twiddy, E. M., and Holmes, R. K. (1992) *Proc. Natl. Acad. Sci. U.S.A. 89*, 7576−7580.
14. Schmitt, M. P., and Holmes, R. K. (1994) *J. Bacteriology 176*, 1141−1149.
15. Posey, J. E., Hardham, J. M., Norris, S. J., and Gherardini, F. C. (1999) *Proc. Natl. Acad. Sci. U.S.A. 96*, 10887−10892.
16. Que, Q., and Helmann, J. D. (2000) *Mol. Microbiol. 35*, 1454−1468.
17. Jakubovics, N. S., Smith, A. W., and Jenkinson, H. F. (2000) *Mol. Microbiol. 38*, 140−153.
18. Hill, P. J., Cockayne, A., Landers, P., Morrissey, J. A., Sims, C. M., and Williams, P. (1998) *Infect. Immun. 66*, 4123−4129.
19. O'Halloran, T. V., Frantz, B., Shin, M. K., Ralston, D. M., and Wright, J. G. (1989) *Cell 56*, 119−129.
20. Chivers, P. T., and Sauer, R. T. (2000) *J. Biol. Chem. 275*, 19735−19741.
21. Chivers, P. T., and Sauer, R. T. (1999) *Protein Sci. 8*, 2494−2500.
22. VanZile, M. L., Cosper, N. J., Scott, R. A., and Giedroc, D. P. (2000) *Biochemistry 39*, 11818−11829.
23. Outten, C. E., Outten, F. W., and O'Halloran, T. V. (1999) *J. Biol. Chem. 274*, 37517−37524.
24. Brocklehurst, K. R., Hobman, J. L., Lawley, B., Blank, L., Marshall, S. J., Brown, N. L., and Morby, A. P. (1999) *Mol. Microbiol. 31*, 893−902.
25. Cook, W. J., Kar, S. R., Taylor, K. B., and Hall, L. M. (1998) *J. Mol. Biol. 275*, 337−346.
26. Morby, A. P., Turner, J. S., Huckle, J. W., and Robinson, N. J. (1993) *Nucleic Acids Res. 21*, 921−925.
27. Patzer, S. I., and Hantke, K. (1998) *Mol. Microbiol. 28*, 1199−1210.
28. Hazlett, K. R. O., Rusnak, F., Kehres, D. G., Bearden, S. W., La Vake, C. J., La Vake, M. E., Maguire, M. E., Perry, R. D., and Radolf, J. D. (2003) *J. Biol. Chem. 278*, 20687−20694.
29. Patzer, S. I., and Hantke, K. (2001) *J. Bacteriol. 183*, 4806−4813.
30. Horsburgh, M. J., Wharton, S. J., Cox, A. G., Ingham, E., Peacock, S., and Foster, S. J. (2002) *Mol. Microbiol. 44*, 1269−1286.
31. Tao, X., Schiering, N., Zeng, H.-Y., Ringe, D., and Murphy, J. R. (1994) *Mol. Microbiol. 14*, 191−197.
32. Guedon, E., and Helmann, J. D. (2003) *Mol. Microbiol. 48*, 495−506.
33. Pace, C. N., Vajdos, F., Fee, L., Grimsley, G., and Gray, T. (1995) *Protein Sci. 4*, 2411−2423.
34. Kuzmic, P. (1996) *Anal. Biochem. 237*, 260−273.
35. Glasfeld, A., Guedon, E., Helmann, J. D., and Brennan, R. G. (2003) *Nat. Struct. Biol., 10*, 652−657.
36. Behlke, J., and Ristau, O. (1997) *Eur. Biophys. J. 25*, 325−332.
37. Kar, S. R., Adam, A. C., Lebowitz, J., Taylor, K. B., and Hall, L. M. (1997) *Biochemistry 36*, 15343−15348.
38. Kar, S. R., Lebowitz, J., Blume, S., Taylor, K. B., and Hall, L. M. (2001) *Biochemistry 40*, 13378−13389.
39. Ralston, G. (1993) *Introduction to Analytical Ultracentrifugation*, Beckman Instruments, Inc., Fullerton.
40. Lakowicz, J. R. (1999) *Principles of Fluorescence Spectroscopy*, Kluwer Academic/Plenum Publishers, New York.

41. Busenlehner, L. S., Weng, T.-C., Penner-Hahn, J. E., and Giedroc, D. P. (2002) *J. Mol. Biol. 319*, 685−701.
42. VanZile, M. L., Chen, X., and Giedroc, D. P. (2002) *Biochemistry 41*, 9776−9786.
43. Connors, K. A. (1987) *Binding Constants: The Measurement of Molecular Complex Stability*, John Wiley & Sons, Inc., New York.
44. Chriswell, C. D., and Schilt, A. A. (1975) *Anal. Chem. 47*, 1623−1629.
45. Tao, X., Zeng, H. Y., and Murphy, J. R. (1995) *Proc. Natl. Acad. Sci. U.S.A. 92*, 6803−6807.
46. Spiering, M. M., Ringe, D., Murphy, J. R., and Marletta, M. A. (2003) *Proc. Natl. Acad. Sci. U.S.A. 100*, 3808−3813.
47. Chen, C. S., White, A., Love, J., Murphy, J. R., and Ringe, D. (2000) *Biochemistry 39*, 10397−10407.
48. Pohl, E., Holmes, R. K., and Hol, W. G. J. (1999) *J. Mol. Biol. 292*, 653−667.
49. Qiu, X., Pohl, E., Holmes, R. K., and Hol, W. G. J. (1996) *Biochemistry 35*, 12292−12302.
50. White, A., Ding, X., vanderSpek, J. C., Murphy, J. R., and Ringe, D. (1998) *Nature 394*, 502−506.
51. Schiering, N., Tao, X., Zeng, H., Murphy, J. R., Petsko, G. A., and Ringe, D. (1995) *Proc. Natl. Acad. Sci. U.S.A. 92*, 9843−9850.
52. Pohl, E., Holmes, R. K., and Hol, W. G. J. (1999) *J. Mol. Biol. 285*, 1145−1156.
53. Lippard, S. J., and Berg, J. M. (1994) *Principles of Bioinorganic Chemistry*, University Science Books, Mill Valley.
54. Kaim, W., and Schwederski, B. (1996) *Bioinorganic Chemistry: Inorganic Elements in the Chemistry of Life*, John Wiley & Sons, Chichester.

BI0350248